Journal of Porphyrins and Phthalocyanines
J. Porphyrins Phthalocyanines 2012; **16**: 370–379
DOI: 10.1142/S1088424612500381

Published at http://www.worldscinet.com/jpp/

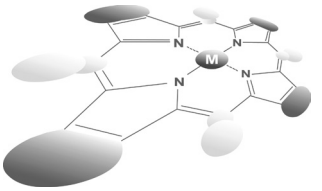

Effect of β-bromo substitution on the photophysical properties of *meso*-phenyl, *meso*-carbazole, and *meso*-triphenylamine porphyrins

Joy E. Haley*[a], Weijie Su[a,b◊], Kristi M. Singh[a,c], Jennifer L. Monahan[a,d], Jonathan E. Slagle[a,e], Daniel G. McLean[a,e] and Thomas M. Cooper[a]

[a] *Materials and Manufacturing Directorate, Air Force Research Laboratory, Wright Patterson Air Force Base, OH 45433, USA*
[b] *General Dynamics Information Technology, Dayton, OH 45431, USA*
[c] *UES, Inc., Dayton, OH 45432, USA*
[d] *Southwestern Ohio Council for Higher Education, Dayton, OH 45420, USA*
[e] *Science Applications International Corporation, Dayton, OH 45431, USA*

Received 27 December 2011
Accepted 14 February 2012

ABSTRACT: We present results of an experimental photophysical study of a series of novel brominated and non-brominated porphyrins that contain phenyl, carbazole, or triphenylamine in the *meso*-position. In addition we have looked at the effects of incorporating a zinc metal into the porphyrin system relative to the free base. Structure-property relationships are established using various absorption and emission techniques including femtosecond pump probe transient absorption and nanosecond laser flash photolysis. With slightly increasing electron donating strength (phenyl < carbazole < triphenylamine) red shifts were observed in all data. The same effect was observed upon the addition of bromine in the beta position. Due to the heavy atom affect of the bromines both the singlet and triplet excited state lifetimes were significantly shorter in the brominated porphyrins. For the T_1–T_n absorption data we observe a large absorption in the near infrared region with the brominated carbazole and triphenylamine. The largest effect of the addition of zinc was in the ground state absorption and emission where a blue shift in the data was observed. Some effects were also observed in the kinetic decays with zinc as the metal compared to the free base porphyrins.

KEYWORDS: triplet excited state, brominated porphyrins, electron donating/withdrawing substitution.

INTRODUCTION

Porphyrins form an important class of chromophores that are being developed and used for many different applications such as photodynamic therapy, commercial dye industry, nonlinear absorption, artificial photosynthesis, oxygen transport, and solar energy conversion [1]. Due to the ease of modification a large amount of effort has gone into developing new porphyrin chromophores that display certain characteristics for certain applications as evidenced by the vast amount of literature on porphyrins [2]. Recently the nonlinear optical properties of porphyrins have been reviewed in detail [3]. The optical properties of the porphyrins along with the vast synthetic methodologies available make porphyrins a target choice for use as nonlinear optical materials. Classes of interest include symmetric and unsymmetric porphyrin, expanded porphyrins, and porphyrin arrays.

Incorporation of electron withdrawing groups (EWG) and electron donating groups (EDG) to the porphyrin core play a large part in altering the electrochemical redox and photophysical properties of porphyrins that have a direct impact on the nonlinearity of a

◊SPP full member in good standing

*Correspondence to: Joy E. Haley, email: Joy.Haley@wpafb.af.mil, tel: +1 (937)-255-9896

material [4–8]. In the work presented here we focus on the structure-property relationships in a series of free base and zinc porphyrins that have been modified in the *meso*-position with either a neutral phenyl or an electron donating triphenylamine or carbazole as well as electron withdrawing octabromination in the *beta* position. By understanding the linear photophysical properties of a series of porphyrins we use this knowledge to better understand the nonlinear properties of a material.

Shown in Fig. 1 are the structures of the 12 chromophores studied. TPP [9], ZnTPP [10], TPOBP [11], and ZnTPOBP [11] are considered model chromophores that have been studied quite a bit in the literature. While TCarbP [12–14], ZnTCarbP [13], TTPAP [15], and ZnTTPAP [15, 16] have appeared in the literature we found no record of the brominated porphyrins TCarbOBP, ZnTCarbOBP, TTPAOBP, and ZnTTPAOBP. In the case of the eight non model porphyrins very little to no excited state data has been obtained. Previously we reported the

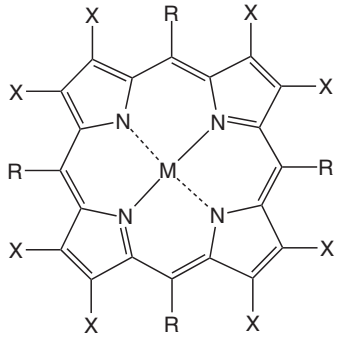

R =	X =	M =	NAME
	H	H_2	TPP
	Br	H_2	TPOBP
	H	Zn	ZnTPP
	Br	Zn	ZnTPOBP
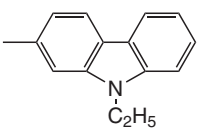	H	H_2	TCarbP
	Br	H_2	TCarbOBP
	H	Zn	ZnTCarbP
	Br	Zn	ZnTCarbOBP
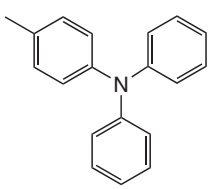	H	H_2	TTPAP
	Br	H_2	TTPAOBP
	H	Zn	ZnTTPAP
	Br	Zn	ZnTTPAOBP

Fig. 1. Shown are the structures of the porphyrins MTPP (5,10,15,20-tetraphenylporphyrin), MTCarbP (5,10,15,20-tetra-9-ethyl-3-carbazolporphyrin), MTTPAP (5,10,15,20-tetratriphenylamine porphyrin), MTPOBP (2,3,7,8,12,13,17,18-octabromo-5,10,15,20-tetraphenylporphyrin), MTCarbOBP (2,3,7,8,12,13,17,18-octabromo 5,10,15,20-tetra-9-ethyl-3-carbazolporphyrin), and MTTPAOBP (2,3,7,8,12,13,17,18-octabromo 5,10,15,20-tetratriphenylamine porphyrin). The M represents either the free base (H_2) or Zn

triplet excited state properties of the model and carbazole series [17]. Here we present a detailed study of both the singlet and triplet excited state properties of these twelve chromophores and how the various groups affect these properties.

EXPERIMENTAL

Materials and synthesis

3,4-Dibromopyrrole was prepared by the reported method [18]. 9-ethyl-3-Carbazolecarboxaldehyde and (4-diphenylamino)benzaldehyde obtained from Aldrich were used as received. TPP and ZnTPP were prepared by Lindsey's method [19].

In this work, we synthesized a series of new *meso*-substituted octabromoporphyrins by one step reaction method which we have previously developed [17]. This synthesis method provides the way to synthesize various *meso*-substituted octabromoporphyrins.

***Meso*-substituted β-octabromoporphyrins.** *Meso*-substituted β-octabromoporphyrins were prepared from 3,4-dibromopyrrole and various aldehydes under Lindsey's conditions. The reactions were performed in dry dichloromethane at room temperature, using BF_3•OEt_2 as the catalyst, followed by oxidation with 2,3-dichloro-5,6-dicyano-l,4-benzoquinone(DDQ). The yield of the *meso*-substituted β-octabromoporphyrins was 15–30%, using suboptimal reaction conditions. Purification was carried out by column chromatography using silica gel and 1:1-3:1 chloroform and hexanes.

Zn(II) complexes of *meso*-substituted β-octabromoporphyrins. The free base β-octabromoporphyrins were dissolved in chloroform or dichloromethane. Zinc acetate dissolved in approximately 1:0.5 chloroform and methanol was then added to the porphyrin solution and stirred at room temperature. Metalation was monitored by UV-vis spectra. After removing the solvent, the purification was carried out by column chromatography using silica gel and chloroform.

Non-brominated *meso*-tetrasubstituted porphyrins. The corresponding *meso*-substituted porphyrins without β-bromosubstitution were synthesized from pyrrole and the respective aldehyde by Lindsey's method.

Zn(II) complexes of non-brominated *meso*-tetrasubstituted porphyrins. The metalation for the nonbrominated porphyrins was similar to that for the brominated ones, except they were run at reflux temperature.

Selected characterization data are as follows

2,3,7,8,12,13,17,18-octabromo-5,10,15,20-tetraphenylporphyrin (TPOBP). ^{1}H NMR (300 MHz; $CDCl_3$): δ, ppm 8.22 (dd, J = 8.1 Hz, J = 1.5 Hz, 8H),

7.82–7.75 (m, 12H), -1.6 (sb, 2H). Anal. calcd. for OBTPP $C_{44}H_{22}Br_8N4$: C, 42.38; H, 1.78; N, 4.49; found C, 42.57; H, 1.89; N, 4.35. MS (MALDI): *m/z* (for $C_{44}H_{22}Br_8N_4$) calcd. 1245.90, found 1246.023. UV-vis (toluene): λ_{max}, nm (log ε) 366 (4.42), 469 (4.91), 566 (3.66), 623 (3.75), 738 (3.53).

Zn(II) 2,3,7,8,12,13,17,18-octabromo-5,10,15,20-tetraphenylporphyrin (ZnTPOBP). ^{1}H NMR (300 MHz; $CDCl_3$): δ, ppm 8.12 (dd, *J* = 7.8 Hz, *J* = 1.5 Hz, 8H), 7.80–7.76 (m, 12H). MS (MALDI): *m/z* (for $ZnC_{44}H_{20}Br_8N_4$) calcd. 1309.28, found 1309.393. UV-vis (toluene): λ_{max}, nm (log ε) 355 (4.36), 471 (5.34), 605 (3.98), 661 (3.96).

5,10,15,20-tetra-9-ethyl-3-carbazolporphyrin (TCarbP). ^{1}H NMR (300 MHz; $CDCl_3$): δ, ppm 8.91 (s, 8H), 8.99 (d, *J* = 1.2 Hz, 4H), 8.39 (d, *J* = 8.4 Hz, 4H), 8.21 (d, *J* = 7.5 Hz, 4H), 7.75 (d, *J* = 8.4 Hz, 4H), 7.59–7.57 (m, 8H), 7.31–7.28 (m, 4H), 4.63 (q, *J* = 7.2 Hz, 8H), 1.68 (t, *J* = 7.2 Hz, 12H), -2.4 (s, 2H). MS (MALDI): *m/z* (for $C_{76}H_{58}N_8$) calcd. 1083.33, found 1083.801. UV-vis (toluene): λ_{max}, nm (log ε) 434 (5.60), 523 (4.19), 563 (4.18), 598 (3.74), 657 (3.82).

Zn(II) 5,10,15,20-tetra-9-ethyl-3-carbazolyl-porphyrin (ZnTCarbP). ^{1}H NMR (300 MHz; $CDCl_3$): δ, ppm 9.01 (s, 8H), 8.97 (s, 4H), 8.40 (d, *J* = 8.4 Hz, 4H), 8.17 (d, *J* = 7.8 Hz, 4H), 7.76 (d, *J* = 8.4 Hz, 4H), 7.58–7.56 (m, 8H), 7.27–7.25 (m, 4H), 4.63 (q, *J* = 7.2 Hz, 8H), 1.68 (t, *J* = 7.2 Hz, 12H). MS (MALDI): *m/z* (for $C_{76}H_{56}N_8Zn$) calcd. 1146.7, found 1146.416. UV-vis (toluene): λ_{max}, nm (log ε) 437 (5.70), 555 (4.39), 597 (4.03).

2,3,7,8,12,13,17,18-octabromo-5,10,15,20-tetra-9-ethyl-3-carbazolyl-porphyrin (TCarbOBP). ^{1}H NMR (300 MHz; $CDCl_3$): δ, ppm 9.03 (dd, *J* = 24 Hz, *J* = 3.5 Hz 4H), 8.49–8.40 (m, 4H), 8.36–8.33 (m, 4H), 7.88 (dd, *J* = 18, *J* = 8.7 4H), 7.65–7.62 (m, 8H), 7.44–7.40 (m, 4H), 4.64 (q, *J* = 6.9 Hz, 8H), 1.69 (t, *J* = 6.9 Hz, 12H), -1.12 (sb, 2H). MS (MALDI): *m/z* (for $C_{76}H_{50}Br_8N_8$) calcd. 1714.5, found 1714.021. UV-vis (toluene): λ_{max}, nm (log ε) 499 (5.27), 671 (3.48), 782 (4.26).

Zn(II)2,3,7,8,12,13,17,18-octabromo-5,10,15,20-tetra-9-ethyl-3carbazolyl-porphyrin (ZnTCarbOBP). ^{1}H NMR (300 MHz; $CDCl_3$): δ, ppm 9.0–8.95 (m, 4H), 8.45–8.36 (m, 4H), 8.36–8.22 (m, 4H), 7.90–7.81 (m, 4H), 7.67–7.64 (m, 4H), 7.62 (d, *J* = 3.6 Hz, 4H), 7.42–7.39 (m, 4H), 4.64 (q, *J* = 6.9 Hz, 8H), 1.70 (t, *J* = 6.9 Hz, 12H). MS (MALDI): *m/z* (for $C_{76}H_{48}Br_8N_8Zn$) calcd. 1777.87, found 1776.958. UV-vis (toluene): λ_{max}, nm (log ε) 496 (5.2), 691 (4.31).

5,10,15,20-tetratriphenylamine porphyrin (TTPAP). ^{1}H NMR (300 MHz; $CDCl_3$): δ, ppm 9.04 (s, 8H), 8.12 (d, *J* = 8.7 Hz, 8H), 7.42–7.46 (m, 40H), 7.15–7.19 (m, 8H), -2.64 (s, 2H). MS (MALDI): *m/z* (for $C_{92}H_{66}N_8$) calcd. 1283.56, found 1283.490. UV-vis (toluene): λ_{max}, nm (log ε) 440 (5.3), 525 (4.17), 567 (4.28), 658 (3.95).

Zn(II) 5,10,15,20-tetratriphenylamine porphyrin (ZnTTPAP). ^{1}H NMR (300 MHz; $CDCl_3$): δ, ppm 9.15 (s, 8H), 8.12 (d, *J* = 8.7 Hz, 8H), 7.45–7.51 (m, 40H), 7.16–7.22 (m, 8H). MS (MALDI): *m/z* (for $ZnC_{92}H_{64}N_8$) calcd. 1346.93, found 1346.367. UV-vis (toluene): λ_{max}, nm (log ε) 442 (5.39), 557 (4.29), 600 (4.08).

2,3,7,8,12,13,17,18-octabromo-5,10,15,20-tetra-triphenylamine porphyrin (TTPAOBP). ^{1}H NMR (300 MHz; $CDCl_3$): δ, ppm 8.07 (d, *J* = 8.4 Hz, 8H), 7.39–7.47 (m, 40H), 7.20–7.23 (m, 8H). MS (MALDI): *m/z* (for $C_{92}H_{58}Br_8N_8$) calcd. 1914.73, found 1914.906. UV-vis (toluene): λ_{max}, nm (log ε) 503 (4.89), 667 (4.29), 775 (4.05).

Zn(II) 2,3,7,8,12,13,17,18-octabromo 5,10,15, 20-tetratriphenylamine porphyrin (ZnTTPAOBP). ^{1}H NMR (300 MHz; $CDCl_3$): δ, ppm 7.96 (d, *J* = 8.4 Hz, 8H), 7.40–7.48 (m, 40H), 7.15–7.19 (m, 8H). MS (MALDI): *m/z* (for $C_{92}H_{56}N_8Zn$) calcd. 1978.09, found 1978.863. UV-vis (toluene): λ_{max}, nm (log ε) 500 (5.0), 682 (4.34).

General techniques

Ground state UV-vis absorption spectra were measured on a Cary 500 spectrophotometer in air-saturated toluene. Emission spectra were measured using a Perkin-Elmer model LS 50B fluorometer. Time-correlated single-photon counting (Edinburgh Instruments OB 920 Spectrometer) was utilized to determine singlet state lifetimes. The sample was pumped with a 70-ps laser diode at 401 nm. Emission was detected on a cooled microchannel plate PMT. Data were analyzed by using a reconvolution software package provided by Edinburgh Instruments.

Ultrafast pump-probe transient absorption measurements were performed using a commercially available femtosecond pump-probe UV-vis spectrometer (HELIOS) purchased from Ultrafast Systems LLC. Briefly, 1-mJ, 150 fs pulses at 800 nm at a 1 KHz repetition rate were obtained from a Ti:sapphire laser (Spectra Physics Hurricane). The output laser beam was split into pump and probe by a beam splitter. The pump beam was directed into a frequency doubler (400 nm) and then focused into the sample. The probe beam was delayed in a computer-controlled optical delay (Newport) and then focused into a sapphire plate to generate white light continuum. The white light was then overlapped with the pump beam in a 2 mm quartz cuvette and then coupled into a CCD detector (Ocean Optics). Data acquisition was controlled by software (Surface Explorer Pro) developed by Ultrafast Systems LLC. The chirp effects were within experimental error, so no chirp corrections were made.

Nanosecond transient absorption measurements were carried out using the third harmonic (355 nm) of a Q-switched Nd:YAG laser (Quantel Brilliant, pulse width *ca*. 5 ns). Pulse fluences of up to 4 $mJ.cm^{-2}$ at the excitation wavelength were typically used. A detailed description of the laser flash photolysis apparatus has

been published earlier [20]. All samples were deoxygenated using a freeze pump thaw method.

Fluorescence quantum yields were determined by using the actinometry method previously described [20]. Zinc *meso*-tetraphenylporphyrin was used as an actinometer with a known fluorescence quantum yield of 0.033 in deoxygenated benzene [21]. All samples were excited at 550 nm with a matched optical density of 0.1.

Computational chemistry

Ground state energy minimizations calculations (DFT, 6-31g(d)/B3LYP) and 20 singlet excited state TDDFT calculations (LANL2DZ/B3LYP) were performed using Gaussian 09 Revision A.02.

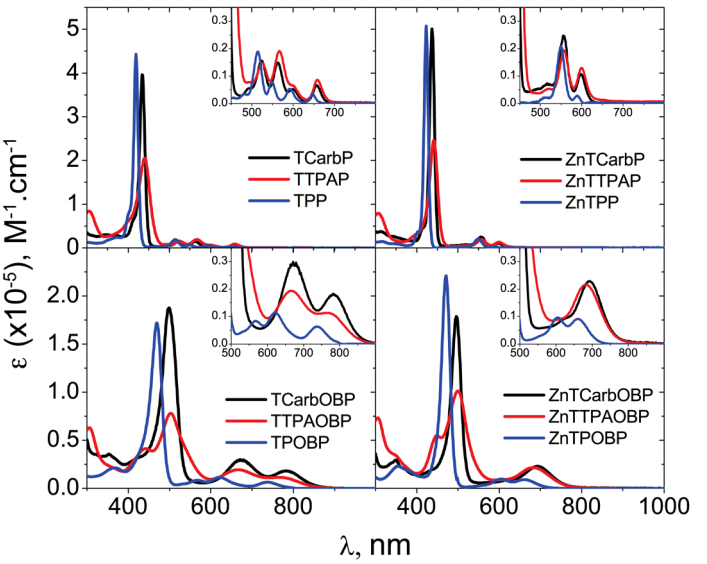

Fig. 2. Ground state absorption of MTPP, MTTPAP, MTCarbP, MTPOBP, MTTPAOBP, MTCarbOBP (M = H_2 or Zn) in air saturated toluene. Molar absorption coefficients are given for the absorbance data. All data were obtained at room temperature

RESULTS AND DISCUSSION

In this work we are interested in establishing structure-property relationships by systematically studying a series of structurally related porphyrins to understand how chemical changes affect the photophysical properties. A series of porphyrins were synthesized that are modified at both the *meso* and *beta* position. At the *meso*-position we look at the effects of a neutral phenyl, electron donating carbazole, and electron donating triphenylamine. At the *beta* position we substitute with either hydrogen or electron withdrawing bromine at all eight positions. The last variation that we are studying is the effect of a metal (M) by comparing the free base (H_2) to porphyrins containing Zn. Shown in Fig. 1 are the structures of the 12 porphyrins studied. The structures are named as follows TPP (5,10,15,20-tetraphenylporphyrin), TTPAP (5,10,15,20-tetratriphenylamine porphyrin), TCarbP (5,10,15,20-tetra-9-ethyl-3-carbazolporphyrin), TPOBP (2,3,7,8,12,13,17,18-octabromo-5,10,15,20-tetraphenylporphyrin), TCarbOBP (2,3,7,8,12,13,17,18-octabromo 5,10,15,20-tetra-9-ethyl-3-carbazolporphyrin), TTPAOBP (2,3,7,8,12,13,17,18-octabromo 5,10,15,20-tetratriphenylamine porphyrin).

Ground state absorbance

Shown in Fig. 2 are the ground state spectra of all the porphyrins in air-saturated toluene. The molar absorption coefficients are given in Table 1. These agree fairly well with available literature data (given in Table 1) in similar solvents for TPP [9], ZnTPP [10], TPOBP [22], ZnTPOBP [23], TTPAP [15], ZnTTPAP [15, 16], TCarbP [13, 14], and ZnTCarbP [13]. There was no data found on TTPAOBP, ZnTTPAOBP, TCarbOBP, and ZnTCarbOBP. Overall the effect of addition of groups at the *meso*-position resulted in a red-shift of the B-band and the Q-band from phenyl to carbazole to triphenylamine. The Q-bands give information about the symmetry of the various complexes. The spectra of the free base porphyrins Q_x and Q_y bands, each split into two vibronic bands, are consistent with D_{2h} symmetry. Upon addition of Zn, the two electronic states become degenerate leaving one state with two vibronic bands, consistent with D_{4h} symmetry. The brominated free base shows two broadened absorption bands, except in the case of TPOBP, where there are three bands, consistent with the known distortion of the chromophore into a saddle shape having C_s symmetry but the Q-bands behave like the chromophore has D_{2h}-like symmetry. Finally, the ZnOBPs have one broad band consistent with a C_s symmetry saddle shape having spectra consistent with D_{2h}-like symmetry. The phenyl group is considered a mostly neutral group while both the carbazole and the triphenylamine behave as full electron donating groups through the resonance effect. Therefore it appears that an electron donating group results in a red-shift. However we must consider the steric effect of these groups and how they lead to increased distortion of the porphyrin [24–28]. These effects are more likely to be causing the red-shift. In all materials containing the triphenylamine we observe a decrease in the intensity of the B-band. The effect of bromination in the *beta* position is quite large. A dramatic red-shift in both the B-band and the Q-band is observed and also a decrease in the intensity of these bands. From the literature it is known that the bromines in this position also act to distort the planarity of the porphyrin, which results in a large red shift [4, 11]. The last comparison is of the free base versus the Zn center. All materials show moderate red-shifting of the B-band with a blue shift of the Q-band with Zn. Also a slight increase in the intensity of these bands with Zn addition is observed.

We analyzed the data according to Gouterman's four orbital model [29]. The B and Q ground state absorption

Table 1. Ground state absorption data

Compound	B-band (0,0)	ε ($M^{-1}.cm^{-1}$)	f (B-band)[a]	Q-band (0,0)	ε ($M^{-1}.cm^{-1}$)	f (Q-band)[a]
TPP	419 nm	442900 ± 11800	1.65	647 nm (648 nm)[b]	3600 ± 100 (3400)[b]	0.12
TCarbP	435 nm (433 nm)[c]	394900 ± 11700 (280000)[c]	1.20	657 nm (655 nm)[c]	5600 ± 400 (5600)[c]	0.15
TTPAP	440 nm (437 nm)[d]	205300 ± 6000 (141000)[d]	1.07	658 nm (659 nm)[d]	8900 ± 100 (7500)[d]	0.20
ZnTPP	423 nm (423 nm)[e]	507400 ± 11000 (544000)[e]	1.58	588 nm (586 nm)[e]	3600 ± 300 (3680)[e]	0.08
ZnTCarbP	437 nm (434 nm)[f]	500600 ± 5100	1.46	598 nm (598 nm)[f]	10700 ± 100	0.11
ZnTTPAP	442 nm (442 nm)[g]	245400 ± 1400 (323600)[g]	1.09	600 nm (603 nm)[g]	12100 ± 100 (15900)[g]	0.11
TPOBP	469 nm (471 nm)[h]	171900 ± 8600 (162200)[h]	1.23	737 nm (740 nm)[h]	6300 ± 300 (5800)[h]	0.12
TCarbOBP	498 nm	193500 ± 2500	1.03	782 nm	18500 ± 400	0.18
TTPAOBP	503 nm	78000 ± 2900	0.84	775 nm	11200 ± 500	0.15
ZnTPOBP	471 nm (472 nm)[i]	228800 ± 2800 (234400)[i]	1.19	661 nm (658 nm)[i]	10700 ± 300 (9800)[i]	0.11
ZnTCarbOBP	496 nm	178800 ± 11700	1.03	691 nm	21100 ± 800	0.31
ZnTTPAOBP	500 nm	102300 ± 1400	0.84	682 nm	22000 ± 400	0.27

[a]Oscillator strengths were calculated from fitting the absorption spectra to Gaussians. [b]In benzene. Literature values from Ref. 9. [c]In chloroform. Literature values from Ref. 14. [d]In dichloromethane. Literature values from Ref. 15. [e]In benzene. Literature values from Ref. 10. [f]In dichloromethane. Literature values from Ref. 13. [g]In toluene. Literature values from Ref. 16. [h]In toluene. Literature values from Ref. 22. [i]In toluene. Literature values from Ref. 23.

bands are interpreted as excitation from the HOMO-1, the HOMO to the LUMO and LUMO+1. When the porphyrin has D_{4h} symmetry, the HOMO-1 and HOMO are nearly degenerate and have representation a_{1u} and a_{2u}, while the LUMO and LUMO+1 are degenerate and have representation e_{gx} and e_{gy}. To calculate B and Q state energy and intensity, configuration interaction is determined between reference B and Q states, given as

$$B_y^0 \equiv (2)^{-1/2}[(a_{2u}e_{gy}) + (a_{1u}e_{gx})] \quad (1)$$

$$Q_y^0 \equiv (2)^{-1/2}[(a_{2u}e_{gy}) - (a_{1u}e_{gx})], \quad (2)$$

with similar expressions for x-polarized states.

The B and Q states are a mixture of the reference states

$$B_y \equiv \cos(\nu)B_y^0 + \sin(\nu)Q_y^0 \quad (3)$$

$$Q_y \equiv -\sin(\nu)B_y^0 + \cos(\nu)Q_y^0 \quad (4)$$

with similar expressions for x-polarized states. The mixing coefficients are determined from the expression

$$\tan(2\nu) \approx \frac{E_{\alpha_{2u}} - E_{\alpha_{1u}}}{E_B - E_Q} \quad (5)$$

where the orbital energies are taken from the calculations and the B and Q state energies taken from experimental measurements.

We used TDDFT to calculate the optical transitions. For many of the compounds the B-bands split into numerous states and no simple analysis was possible. The Q-bands were straightforward to analyze. Table 2 lists the calculated Q states, their composition, energy and oscillator strength. Figure 3 is a plot of calculated *vs.* experimental Q(0,0) band energy. There is a reasonable correlation although our calculations tend to overestimate the energy. The traditional four level model describes optical transitions in porphyrins as arising from the HOMO-1 and HOMO to the LUMO and LUMO+1. The Q-bands of many of these compounds did not follow this simple pattern. For example the Q-band of TTPAP involves transitions from HOMO-5 to LUMO. Examination of the molecular orbitals and a comparison show the HOMO of all the compounds has "a_{2u}-like" appearance even when the overall chromophore has a lower symmetry. Similarly, the LUMO and LUMO+1 have "e_g-like" appearance. Finally, each chromophore has an "a_{1u}-like" (for example the HOMO-5 of TTPAP) orbital from which there are transitions to the "e_g-like" orbitals. An exception is ZnTTPAOBP where the Q-band is a HOMO to LUMO transition and the HOMO is localized on the triphenyl amine ligand, suggesting the transition has charge transfer character. Table 3 lists the energies of these orbitals. The quantity Tan(2ν) was calculated from these energies and the experimental Q and B-band energies. For all compounds Tan(2ν) varies as Phenyl < Carb < TPA, showing the increasing ligand size causes increasing

Table 2. Calculated Q-band data

Compound	State	Composition[a]	E, eV	f[b]
TPP	B_{2u}	0.57 (***H-1*** → L+1), 0.82 (H → L)	2.21	0.021
TPP	B_{3u}	-0.62 (***H-1*** → L), 0.78 (H → L+1)	2.38	0.056
TCarbP	B	0.18 (H-5 → L+1), -0.52 (***H-1*** → L+1), 0.83 (H → L)	2.15	0.056
TCarbP	A	-0.16 (H-5 → L), 0.56 (***H-1*** → L), 0.81 (H → L+1)	2.31	0.084
TTPAP	A_u	0.44 (***H-5*** → L+1), 0.89 (H → L)	2.07	0.14
TTPAP	B_u	-0.41 (***H-5*** → L), 0.91 (H → L+1)	2.20	0.22
ZnTPP	E_u	0.63 (***H-1*** → L), 0.76 (H → L+1)	2.36	0.0089
ZnTPP	E_u	-0.63 (***H-1*** → L), 0.76 (H → L+1)	2.38	0.0089
ZnTCarbP	A	0.26 (***H-1***→ L), -0.53 (***H-1*** → L+1), 0.72 (H → L), 0.35 (H → L+1)	2.30	0.052
ZnTCarbP	A	0.53 (***H-1*** → L), 0.26 (***H-1*** → L+1), -0.35 (H → L), 0.72 (H → L+1)	2.30	0.052
ZnTTPAP	B_u	-0.47 (***H-5*** → L), 0.87 (H → L+1)	2.22	0.14
ZnTTPAP	A_u	0.46 (***H-5*** → L), 0.88 (H → L+1)	2.22	0.14
TPOBP	B_2	0.50 (***H-1*** → L+1), 0.86 (H → L)	1.91	0.049
TPOBP	B_1	-0.57 (***H-1*** → L), 0.82 (H → L+1)	2.08	0.053
TCarbPOBP	B	-0.28 (***H-6*** → L+1), 0.28 (***H-5*** → L+1), 0.91 (H → L)	1.85	0.19
TCarbPOBP	B	0.28 (***H-6*** → L), -0.33 (***H-5*** → L), -0.19 (H-1 → L), 0.88 (H → L+1)	2.03	0.21
TTPAOBP	A″	0.23 (***H-5*** → L+1), 0.97 (H → L)	1.65	0.28
TTPAOBP	A′	-0.17 (***H-5*** → L), -0.48 (H-1 → L), 0.85 (H → L+1)	1.77	0.43
ZnOBP	E	-0.57 (***H-1*** → L+1), 0.81 (H → L)	2.13	0.040
ZnOBP	E	0.57 (***H-1*** → L), 0.81 (H → L+1)	2.13	0.040
ZnTCarbPOBP	E	-0.45 (***H-5*** → L+1), -0.16 (H-1 → L+1), 0.84 (H → L), 0.21 (H → L+1)	2.05	0.14
ZnTCarbPOBP	E	0.45 (***H-5*** → L), 0.16 (H-1 → L), -0.21 (H → L), 0.84 (H → L+1)	2.05	0.14
ZnTTPAPOBP[c]	A′	0.19 (***H-5***→ L+1), 0.97 (H → L)	1.77	0.25
ZnTTPAPOBP	A″	-0.19 (***H-5*** → L), 0.97 (H → L+1)	1.77	0.26

[a]The porphyrin ring orbitals for the energy level labeled in ***bold italic*** have a_{1u}-like symmetry. [b]Oscillator strength. [c]The HOMO of ZnTTPAPOBP is localized on the triphenyl amine ligand.

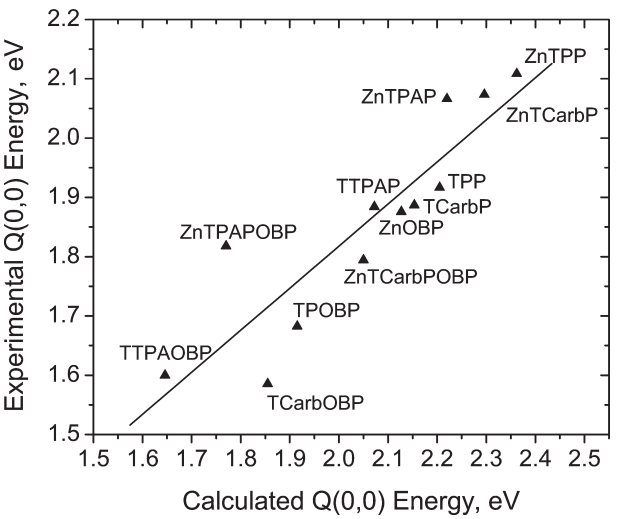

Fig. 3. Plot of observed Q(0,0) state energy *vs.* calculated Q(0,0) energy

mixing of the B^0 and Q^0 reference states. Figure 4 is a plot of measured B and Q-band oscillator strength *vs.* Tan(2ν). The trend suggests that as the mixing of B^0 and Q^0 reference states increases, the B-band loses intensity and the Q-band gains intensity.

Table 3. List of Gouterman orbital energies used in analysis of spectroscopic data

Compound	E(a_{1u}-like orbital), eV	E(a_{2u}-like orbital), eV	Tan(2ν)
TPP	-5.4853	-5.1397	0.33136
TCarbP	-5.3329	-4.9680	0.37889
TTPAP	-5.4420	-4.8417	0.64300
ZnTPP	-5.3985	-5.1677	0.28055
ZnTCarbP	-5.2624	-4.9862	0.36158
ZnTTPAP	-5.3596	-4.8670	0.66678
TPOBP	-5.7919	-5.3375	0.47272
TCarbOBP	-5.9285	-5.2643	0.73463
TTPAOBP	-5.9900	-5.0371	1.1015
ZnTPOBP	-5.9824	-5.5963	0.51031
ZnTCarbOBP	-5.8815	-5.3650	0.73216
ZnTTPAOBP	-5.9582	-5.0913	1.3101

Fluorescence

Typical S_1–S_0 emission from both series of porphyrins is shown in Fig. 5. The spectral data is consistent with literature data for TPP [21], ZnTPP [21], TPOBP [11], ZnTPOBP [11], ZnTTPAP [16], TCarbP [12], and ZnTCarbP [13]

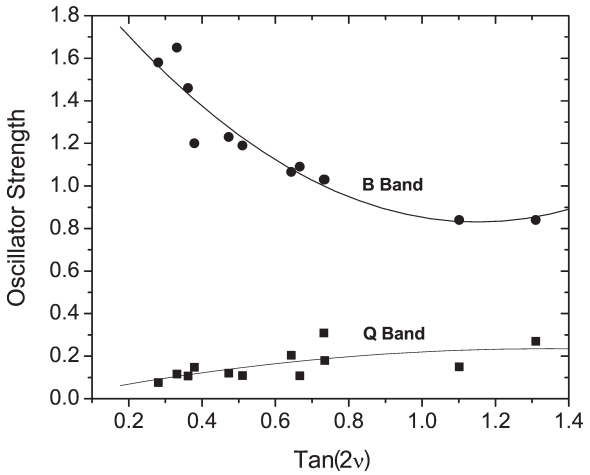

Fig. 4. Plot of B and Q-band oscillator strength *vs.* calculated Tan(2ν)

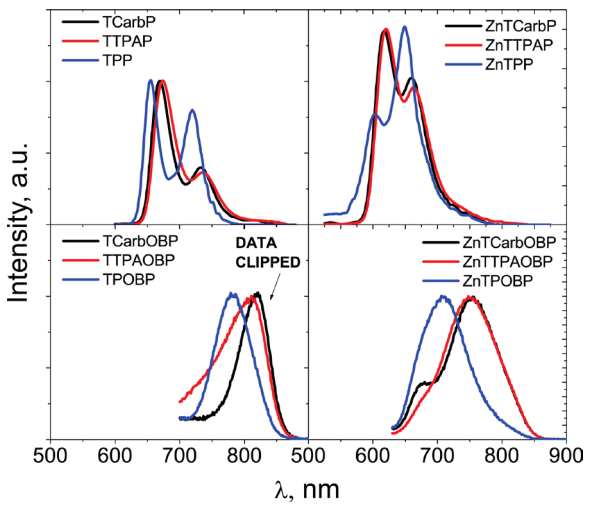

Fig. 5. Emission of MTPP, MTTPAP, MTCarbP, MTPOBP, MTTPAOBP, and MTCarbOBP in air saturated toluene. Samples were excited at 550 nm. The data for TCarbOBP and TTPAOBP is clipped due to limitations of the detector beyond 850 nm but shows a portion of the emission

in similar solvents (Table 4). The data for TCarbOBP and TTPAOBP are slightly clipped due to limitations of our detector in this region. Therefore we do not know the peak maximum for these two porphyrins but assume that they are lower in energy. The fluorescence quantum yields (Φ_F) were determined using *meso*-tetraphenylporphyrin (ZnTPP) as a standard with a known quantum yield of 0.033 in deaerated benzene and are given in Table 4 [21]. These values are also consistent with literature data given in Table 4 for TPP [21], ZnTPP [21], TCarbP [12], and ZnTCarbP [13]. The addition of the group in the *meso*-position results in moderate red-shifting of the fluorescence with a slight increase in the fluorescence quantum yield for the non-brominated porphyrins. The largest effect is observed upon the addition of the bromines in the *beta* position. We see quite large red-shifting that is consistent with the absorption spectra. We also found a much smaller fluorescence quantum yield for these materials compared to the others. The effect of adding the Zn resulted in blue-shifting of the emission, which is consistent with the absorbance data and an overall smaller fluorescence quantum yield. The singlet excited state lifetime was also monitored using time correlated single photon counting. The results are given in Table 4 and are all obtained under air saturated conditions. Our data is similar to data obtained in the literature (Table 4) for TPP [21], ZnTPP [21], and ZnTTPAP [16] in similar solvents. Consistent with much smaller fluorescence quantum yields a significantly shorter singlet lifetime for the brominated species is observed compared to the non-brominated. This is due to increased intersystem crossing to the triplet excited state because of an internal heavy atom effect of the added bromines. The lifetimes of the free-base versus Zn porphyrins are consistent with the fluorescence quantum yields.

S_1–S_n absorption

The singlet excited state absorbance was probed using a femtosecond pump-probe experiment. The samples were

Table 4. Singlet excited state photophysical properties of porphyrins in toluene

Compound	Fl Q (0,0)	τ_S TCSPC[a]	Φ_{fl}[a]	E_s, eV	S_1–S_n max
TPP	656 nm (652 nm)[b]	9.9 ns (13.6 ns)[b]	0.078 (0.11)[b] 0.102[b]	1.91	451 nm
TCarbP	669 nm (665 nm)[c]	8.7 ns	0.198 (0.215)[c]	1.87	469 nm
TTPAP	674 nm	8.5 ns	0.216	1.86	479 nm
ZnTPP	601 nm (598 nm)[b]	2.1 ns (2.7 ns)[b]	0.034 (0.033)[b]	2.09	459 nm
ZnTCarbP	618 nm (615 nm)[d]	1.5 ns	0.060 (0.087)[d]	2.05	473 nm
ZnTTPAP	620 nm	1.5 ns (2.66 ns)[e]	0.074	2.04	471 nm
TPOBP	783 nm (762 nm)[f]	<50 ps	~0.0009	1.64	498 nm
TCarbOBP	>820 nm	<50 ps	>0.0002	1.54	549 nm
TTPAOBP	>810 nm	63 ps	>0.0005	1.57	591 nm
ZnTPOBP	735 nm (728 nm)[f]	<50 ps	~0.0006	1.81	503 nm
ZnTCarbOBP	773 nm	80 ps	~0.0015	1.69	532 nm
ZnTTPAOBP	778 nm	104 ps	~0.0018	1.70	559 nm

[a]Samples are air saturated. [b]In deoxy benzene. Literature values from Ref. 21. [c]In THF. Literature values from Ref. 12. [d]In toluene. Literature values from Ref. 13. [e]In toluene. Literature values from Ref. 16. [f]In chloroform. Literature values from Ref. 11.

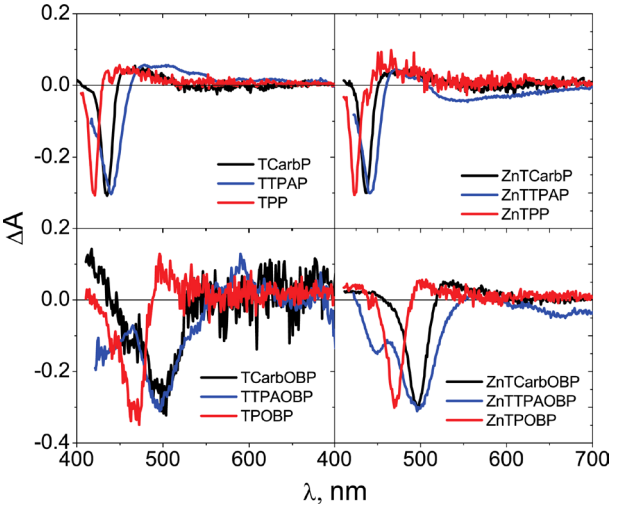

Fig. 6. Singlet excited state absorbance data (S_1–S_n) observed after femtosecond pulsed excitation at 400 nm of MTPP, MTTPAP, MTCarbP, MTPOBP, MTTPAOBP, and MTCarbOBP in air saturated toluene

excited at 400 nm with a 150 fs pulse and monitored from 420–800 nm. These data are given in Fig. 6 immediately following the laser pulse and the maximum is given in Table 4. These data have been normalized at the bleaching peak for comparison. Unfortunately some of the data are noisier due to a small signal. Consistent with the ground state absorbance data a red-shift in the peak maximum is observed with addition of the carbazole and amine groups in the *meso*-position. Also the effect of bromination in the *beta* position is a red-shift of the peak maximium. Lastly the addition of Zn showed very little effect to the peak maximum of these data indicating that the central metal does not play a role in the S_1–S_n absorption.

Careful analysis of the kinetic decays associated with each porphyrin upon femtosecond excitation show several lifetimes prior to intersystem crossing to the triplet state as given in Table 5. Also given in Table 5 in parenthesis are ultrafast lifetimes taken from the literature for TPP and ZnTPP in benzene [30, 31]. The first lifetime (τ_1) is almost undoubtedly due to IVR (intramolecular vibrational redistribution). This is due to relaxation from upper vibrational levels in both the S_2 and S_1 states down to the lowest vibrational level of the S_1 state. This generally occurs on a < 1 ps time scale. It is observed in all 12 chromophores. For TPP our τ_1 value agrees very well with the literature but for ZnTPP our decay is much faster than the literature value [30, 31]. For the non-brominated porphyrins and ZnTTPAOBP the second lifetime (τ_2) is believed to be due to elastic collisions of solvent and solute or solvent induced vibrational energy redistribution. For both TPP and ZnTPP our data is within error of those previously measured [30, 31]. For the brominated porphyrins except for ZnTTPAOBP the second lifetime is assigned to intersystem crossing to the triplet excited state. These lifetimes are in agreement with the TCSPC data given in Table 4. For TPP we observe a third lifetime that is attributed to solvent induced vibrational energy redistribution caused by energy exchange collisions leading to thermal equilibrium with the solvent [30]. In the case of the non-brominated porphyrins except TPP and ZnTTPAOBP we observed a third lifetime (τ_3) that we attribute to intersystem crossing to the triplet excited state. These lifetimes were obtained from the TCSPC data in air saturated benzene due to their long decays. For ZnTTPAOBP the lifetime from femtosecond transient absorption (86 ps) is consistent with the lifetime measured using TCSPC of 100 ps. For TPP intersystem crossing is associated with τ_4 of near 10 ns in air saturated toluene.

Looking for trends in the singlet excited state data show that intersystem crossing is rapid in the brominated porphyrins and competes with any possible elastic collisions of solvent and solute. This is expected due to the heavy atom effect of the bromines. For ZnTTPAOBP we do observe a lifetime associated with solvent and

Table 5. Singlet lifetimes of porphyrins in air saturated toluene

Compound	τ_1	τ_2	τ_3	τ_4
TPP	220 ± 140 fs (200 fs)[a]	3.8 ± 1.3 ps (1.4 ps)[a]	23 ± 4 ps (10–20 ps)[a]	9.9 ± 0.1 ns
TCarbP	270 ± 300 fs	22 ± 17 ps	8.7 ± 0.2 ns	—
TTPAP	660 ± 800 fs	59 ± 33 ps	8.5 ± 0.1 ns	—
ZnTPP	220 ± 290 fs (1.5 ps)[b]	23 ± 13 ps (12 ps)[b]	2.1 ± 0.2 ns	—
ZnTCarbP	1.2 ± 1.5 ps	22 ± 12 ps	1.5 ± 0.1 ns	—
ZnTTPAP	100 ± 30 fs	13 ± 10 ps	1.5 ± 0.1 ns	—
TPOBP	1.8 ± 2.3 ps	36 ± 25 ps	—	—
TCarbOBP	960 ± 940 fs	21 ± 14 ps	—	—
TTPAOBP	1.8 ± 1.5 ps	75 ± 23 ps	—	—
ZnTPOBP	740 ± 540 fs	19 ± 12 ps	—	—
ZnTCarbOBP	300 ± 170 fs	28 ± 21 ps	—	—
ZnTTPAOBP	590 ± 420 fs	9.0 ± 6.5 ps	86 ± 29 ps	—

[a]In benzene. Literature values from Ref. 30. [b]In benzene. Literature values from Ref. 31.

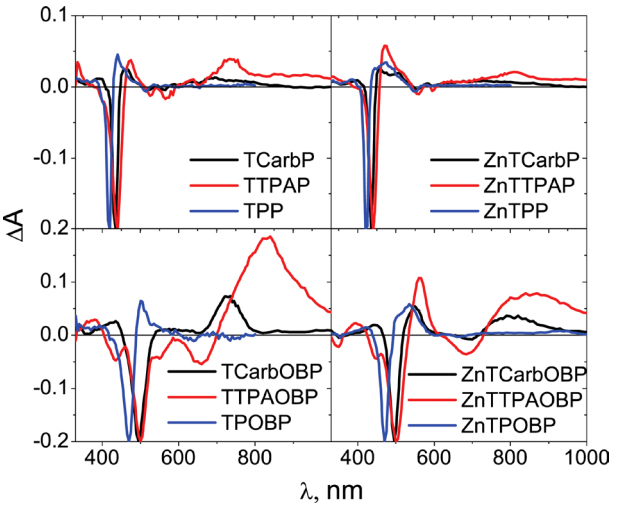

Fig. 7. Triplet excited state absorbance data (T_1–T_n) observed after nanosecond pulsed excitation (at the B-band) of MTPP, MTTPAP, MTCarbP, MTPOBP, MTTPAOBP, and MTCarbOBP in deoxygenated toluene

solute relaxation collisions. Also for this particular chromophore the intersystem crossing lifetime is nearly twice as slow as ZnTPOBP and ZnTCarbOBP. The same is true for TTPAOBP compared to TPOBP and TCarbOBP. This suggests that the triphenlyamine group in the *meso*-position is pulling the electron density away from the bromine atoms that induce the heavy atom effect.

For the series of non-brominated porphyrins the addition of the carbazole or triphenylamine group appear to shorten the lifetime associated with intersystem crossing suggesting that triplet formation is slightly larger in these chromophores. Also as expected the non-brominated porphyrins containing zinc have a shorter singlet excited state lifetime due to increased intersystem crossing to the triplet excited state compared to the free base porphyrins.

T_1–T_n absorption

The triplet excited state spectra given in Fig. 7 were obtained by exciting with a 4 ns pulse at the B-band peak wavelength for each sample. All samples were deoxygenated by three freeze-pump-thaw cycles. For clarity in comparison the data have been normalized at the bleaching peak. The peak maxima and deoxygenated lifetimes are given in Table 6. We also obtained the triplet excited state lifetimes under air saturated conditions and have included this data in Table 6 for comparison. For the non-brominated porphyrins the triplet lifetimes under deoxygenated conditions are significantly longer indicating that oxygen is quenching the triplet excited state. For the brominated series the lifetimes obtained under both air saturated and deoxygenated conditions are within error of each other except for ZnTCarbOBP and ZnTTPAOBP. Due to the slight difference in the latter two porphyrins some oxygen quenching is occurring but in general the lifetimes are still significantly shorter than the non-brominated porphyrins. As intersystem crossing to the triplet excited state increases a shortening of the triplet lifetime is observed suggesting that the brominated series have larger intersystem crossing quantum yields. At this time we have not determined the intersystem crossing quantum yields for the series of porphyrins presented here.

Comparing the spectral data a few trends are observed. The most notable effect of addition of the carbazole or amine in the *meso*-position is the large increase in

Table 6. Triplet excited state photophysical properties of porphyrins in toluene

Compound	T_1–T_n max	τ_T[a]	τ_T[b]
TPP	440 nm (790 nm)[c]	217 ± 26 μs (1500 μs)[c]	331 ± 4 ns
TCarbP	465 nm	306 μs	333 ± 11 ns
TTPAP	470 nm	198 ± 2 μs	308 ± 9 ns
ZnTPP	475 nm (845 nm)[c]	233 ± 23 μs	526 ± 46 ns
ZnTCarbP	455 nm	297 ± 80 μs	633 ± 25 ns
ZnTTPAP	475 nm	202 ± 23 μs	718 ± 22 ns
TPOBP	500 nm (520 nm)[d]	189 ± 51 ns (130 ns)[d]	146 ± 4 ns
TCarbOBP	725 nm	148 ± 22 ns	166 ± 16 ns
TTPAOBP	840 nm	161 ± 9 ns	152 ± 8 ns
ZnTPOBP	535 nm (540 nm)[d]	269 ± 48 ns (110 ns)[d]	200 ± 30 ns
ZnTCarbOBP	545 nm	1.2 ± 0.1 μs	508 ± 21 ns
ZnTTPAOBP	565 nm	524 ± 29 ns	200 ± 19 ns

[a]Samples deoxygenated by three freeze pump thaw cycles. [b]Samples are air saturated. [c]In deoxygenated benzene. Literature values from Ref. 21. [d]In deoxygenated dioxane.
Venanzi M, Tagliatesta P, Pastorini A, Mari P, Elisei F, Latterini L and Kadish KM. *J. Porphyrins Phthalocyanines* 2002; **6**: 643.

absorption in the region from 700–1000 nm. For the brominated versions this increase is quite significant relative to the bleaching peak. Also observed is a progressive red-shift in the maximum with the addition of the electron donating groups.

CONCLUSION

Overall the data presented in this work reveals that incorporation of increasing electron donating groups in the *meso*-position does not have a huge effect on the overall photophysical properties. We do observe some red-shifting of the absorbance and emission data. However the incorporation of the eight bromine groups in the beta position does show significant effects mainly with the kinetic decay data. We attribute these effects to mainly the heavy atom effect of the bromine to induce intersystem crossing to the triplet excited state but cannot rule out distortion effects of the macrocycle.

Acknowledgements

We are thankful for the support of this work by AFRL/RX contracts FA8650-04-C-5410 for D.G.M. and J.E.S. and FA8650-09-D-5430 for K.M.S., and W.S. We would also like to thank Dr. Aaron R. Burke for NMR characterization.

REFERENCES

1. Milgrom LR. *The Colours of Life*, Oxford University Press: Oxford, 1997.
2. *The Porphyrin Handbook*, Kadish KM, Smith KM and Guilard R. (Eds.) Academic Press: San Diego, 2000.
3. Senge MO, Fazekas M, Notaras EGA, Blau WJ, Zawadzka M, Locos OB and Mhuircheartaigh EMN. *Adv. Mater.* 2007; **19**: 2737.
4. Senge MO, Gertsung V, Ruhlandt-Senge K, Runge S and Lehmann I. *J. Chem. Soc. Dalton Trans*. 1998; 4187.
5. Duval H, Bulach V, Fischer J and Weiss R. *Inorg. Chem*. 1999; **38**: 5495.
6. Leroy J, Porhiel E and Bondon A. *Tetrahedron* 2002; **58**: 6713.
7. Bhyrappa P, Sankar M and Varghese B. *Inorg. Chem*. 2006; **45**: 4136.
8. Heinze K and Reinhart A. *Dalton Trans*. 2008; 469.
9. Barnett GH, Hudson MF and Smith KM. *J. Chem. Soc. Perkin Trans. I* 1975; 1401.
10. Quimby DJ and Longo FR. *J. Am. Chem. Soc*. 1975; **97**: 5111.
11. Bhyrappa P and Krishnan V. *Inorg. Chem*. 1991; **30**: 239.
12. Xu TH, Lu R, Qiu XP, Liu XL, Xue PC, Tan CH, Bao CY and Zhoa YY. *Eur. J. Org. Chem*. 2006; 4014.
13. Walsh CJ, Sooksimuang T and Mandal BK. *J. Poprhyrins Phthalocyanines* 2001; **5**: 803.
14. Tidwell CP, Alexander LA, Fondren LD, Belmore K and Niles DE. *Indian J. Chem. B: Org. Chem. Med. Chem*. 2007; **46B**: 1658.
15. Huang C-W, Chiu KY and Cheng S-H. *J. Chem. Soc. Dalton Trans*. 2005; 2417.
16. Fu S, Zhu X, Zhou G, Wong W-Y, Ye C, Wong W-K and Lis Z. *Eur. J. Inorg. Chem*. 2007; 2004.
17. Su W, Singh K, Rogers J, Slagle J and Fleitz P. *Mater. Sci. Eng. B* 2006; **132**: 12.
18. Bray BL, Mathies PH, Naef R, Solas DR, Tidwell TT, Aris DR and Muchowiski JM. *J. Org. Chem*. 1990; **55**: 6317.
19. Lindsey JS, Schrieman IC, Hsu HC, Keamey PC and Marguerettaz AM. *J. Org. Chem*. 1987; **52**: 827.
20. Rogers JE, Cooper TM, Fleitz PA, Glass DJ and McLean DG. *J. Phys. Chem. A* 2002; **106**: 10108.
21. Lee WA, Gratzel M and Kalyanasundaram K. *Chem. Phys. Lett*. 1984; **108**: 308.
22. Bhyrappa P and Bhavana P. *Chem. Phys. Lett*. 2001; **342**: 39.
23. Bhyrappa P, Krishnan V and Nethaji M. *J. Chem. Soc. Dalton Trans*. 1993; 1901.
24. Senge MO. In *The Porphyrin Handbook*, Vol. 1, Kadish KM, Smith KM and Guilard R. (Eds.) Academic Press: Boston, 2000; pp 239.
25. Wertsching AK, Koch AS and DiMagno SG. *J. Am. Chem. Soc*. 2001; **123**: 3932.
26. Ryeng H and Ghosh A. *J. Am. Chem. Soc*. 2002; **124**: 8099.
27. Haddad RE, Gazeau S, Pecaut J, Marchon J-C, Medforth CJ and Shelnutt JA. *J. Am. Chem. Soc*. 2003; **125**: 1253.
28. Golubchikov OA, Pukhovskaya SG and Kuvshinova EM. *Russian Chem. Rev*. 2005; **74**: 249.
29. a) Gouterman M. *J. Chem. Phys*. 1959; **30**: 1139. b) Gouterman M. *The Porphyrins*, Vol. III, Academic Press: New York, 1978; pp 1.
30. Baskin JS, Yu H-Z and Zewail AH. *J. Phys. Chem. A* 2002; **106**: 9837.
31. Yu H-Z, Baskin JS and Zewail AH. *J. Phys. Chem. A* 2002; **106**: 9845.